Model of the cAMP activation of chloride transport by CFTR channel and the mechanism of potentiators

Oscar Moran

www.elsevier.com/locate/yjtbi

Model of the cAMP activation of chloride transport by CFTR channel and the mechanism of potentiators

Oscar Moran

PII: S0022-5193(09)00406-8
DOI: doi:10.1016/j.jtbi.2009.08.032
Reference: YJTBI 5685

To appear in: *Journal of Theoretical Biology*

Received date: 23 July 2009
Revised date: 12 August 2009
Accepted date: 22 August 2009

Cite this article as: Oscar Moran, Model of the cAMP activation of chloride transport by CFTR channel and the mechanism of potentiators, *Journal of Theoretical Biology*, doi:10.1016/j.jtbi.2009.08.032

Model of the cAMP activation of chloride transport by CFTR channel and the mechanism of potentiators

Oscar Moran

Istituto di Biofisica, CNR. Via De Marini, 6, 16149 Genova, Italy. moran@ge.ibf.cnr.it

Mutations of the cystic fibrosis transmembrane conductance regulator (CFTR) cause cystic fibrosis, a hereditary lethal disease. CFTR is a chloride channel expressed in the apical membrane of epithelia. It is activated by cAMP dependent phosphorylation and gated by the binding of ATP. The impaired chloride transport of some types of cystic fibrosis mutations could be pharmacologically solved by the use of chemical compounds called potentiators. Here it is undertaken the construction of a model of the CFTR activation pathways, and the possible modification produced by a potentiator application. The model yields a novel mechanism for the potentiator action, describing the activatory and inhibitory activities on two different positions in the CFTR activation pathway.

1. Introduction

The cystic fibrosis transmembrane conductance regulator (CFTR) is an integral membrane protein that forms an ATP-gated anion channel activated by a cAMP-dependent phosphorylation. CFTR is responsible for the chloride and bicarbonate permeability on the apical membrane of most epithelia. Its activity is modulated by the intracellular concentration of cAMP, in turn, regulated by extracellular stimulus by several hormone receptors. It has been proposed that CFTR cAMP-dependent phosphorylation may be modulated by cAMP-dependent protein kinase (Kongsuphol et al., 2009; King et al., 2009) and by phosphorylation of CFTR by protein kinase-C (Button et al., 2001; Chappe et al., 2004; Seavilleklein et al., 2009).

Mutations of the gene coding for CFTR produce cystic fibrosis (CF), an autosomic recessive lethal disease. Defects on CFTR may result on a lack of the protein, because of a premature stop codon (class 1), fault in the CFTR traffic with a consequent degradation of the protein before reaching the plasma membrane (class 2), or impaired ion transport because of defects on the gating mechanism (class 3) or in the permeation pathway (class 4). In an attempt to increase the ion transport in defective CFTR, several molecules, called potentiators, have been identified (for a review, see Galietta and Moran, 2004). These molecules have been proposed to be potentially useful for CF treatment on patients with class 3 and 4 mutations, and probably also for patients carrying the most

common mutation, dF508, a class 2 mutations that, after been pharmacologically rescued, may present a reduced ion transport.

Most research to find more effective potentiators have been done by "brute force" methods, like high throughput screening, or by studying the properties of analogues of already known putative potentiators. A more "intelligent" design of drugs has not been tried because of the lack of informations about the precise target for drugs, either in terms of a well identified binding site based on direct structural data, or by the insufficient knowledge on the precise step on the activation and gating pathways that determine the CFTR function.

In this work I have attempted to construct a model of the pathways that lead to the activation of CFTR upon an increase of intracellular cAMP. The interest to describe the system as a function of cAMP concentration is because this parameter is currently used when CFTR physiology or pharmacology is studied on cell monolayers, applying either a permeable cAMP analogue, or activating the adenylate cyclase by forskolin (Moran and Zegarra-Moran, 2005, 2008). I have designed the model putting together data describing several sections of the complete pathway. The model is described in steady-state conditions, as most transitions on these pathways may occur with relaxation times (between 10^{-6}-10 s) faster than the time course of the anion transport with physiological meaning (>1 min), rendering irrelevant the kinetics of these events.

2. The model

A general scheme of the activation of CFTR is presented in figure 1. When an extracellular ligand binds a receptor there is an increase of intracellular cAMP by the activation of adenylate cyclase, that binds the PKA-holoenzyme. Activation of CFTR occurs upon PKA-dependent phosphorylation of CFTR, and gating of the CFTR-channels comes after binding of ATP.

2.1 Activation of PKA

Activation of PKA occurs when the catalytic subunit (C) dissociates from the regulatory subunit (R) upon binding of 4 molecules of cAMP to R:

$$\begin{matrix} R-C \\ | \quad | \\ R-C \end{matrix} + 4cAMP \rightleftharpoons \begin{matrix} cAMP\text{-}R\text{-}cAMP \\ | \\ cAMP\text{-}R\text{-}cAMP \end{matrix} + \begin{matrix} C \\ | \\ C \end{matrix}$$

The binding of cAMP to the isoform RIα of the PKA holoenzyme has been recently described by

Dao et al. (2006) with a second order dissociation constant, K_d, of 2.9 μM. Hence, the probability to be active at steady-state, PKA_A, is expressed by:

$$PKA_A = \left(\frac{[cAMP]}{K_d + [cAMP]} \right)^{n_p} \quad (1)$$

where $[cAMP]$ is the concentration of the nucleotide, and $n_p = 4$ depicts the probability that all four cAMP-binding sites have to be occupied to activate the enzyme. When activated, PKA catalyses the phosphorylation of serine residues in the regulatory domain of CFTR.

2.2 cAMP dependent phosphorylation of CFTR: Activatory sites

The regulatory domain of the CFTR has 12 to 14 putative phosphorylation sites (Seibert et al, 1999). Probably 9 of the phosphorylation sites are activatory, and at least 4 sites need to be phosphorylated to get an active CFTR (Chang et al, 1993). Other 3 putative sites that inhibit the CFTR when phosphorylated (Csanady et al 2005). For this model, I assume there are two independent and separate parallel phosphorylation pathways. The first one includes 9 transitions activatory states, and the second is a 3 transitions inhibitory pathway. A phosphorylation step is described as a second order reaction, where the forward reaction is catalysed by the activated PKA, and the backward reaction is driven by phosphatases.

$$\text{CFTR} + \text{ATP} \underset{\text{phosphatase}}{\overset{\text{PKA}_\text{A}}{\rightleftharpoons}} \text{CFTR-P} + \text{ADP}$$

Assuming that, at equilibrium, dephosphorylation proceeds at a constant rate, the amount of phosphorylated sites in a protein will depend on the activity of the PKA. Thus, the equilibrium constants for the phophorylation step, K_{Fa} and K_{Fi}, defined for the activation and inhibition pathways, is expressed as:

$$K_{Fx} = \frac{k_{PKA}}{k_{phosphatase}} \quad (2)$$

where k_{PKA} and $k_{phosphatase}$ are the rate constants for the forward (PKA-dependent phosphorylation) and backward (phosphatase-dependent dephosphorylation) transitions, respectively. The effective equilibrium constant, $K_{Fx,eff}$, is then expressed as:

$$K_{Fx,eff} = \frac{1}{K_{Fx} \times PKA_A \times \left(\frac{[ATP]}{[ATP] + K_p} \right)} \quad (3)$$

where K_P is the second order equilibrium constant of the PKA catalysed phosphorylation and [*ATP*] is the nucleotide concentration. Intracellular ATP concentration could be estimated as 4.7 mM (James et al. 1999), and K_p is 0.0093 mM (Zu et al. 1994). The sequence of phosphorylation steps on the CFTR activation pathway is described by:

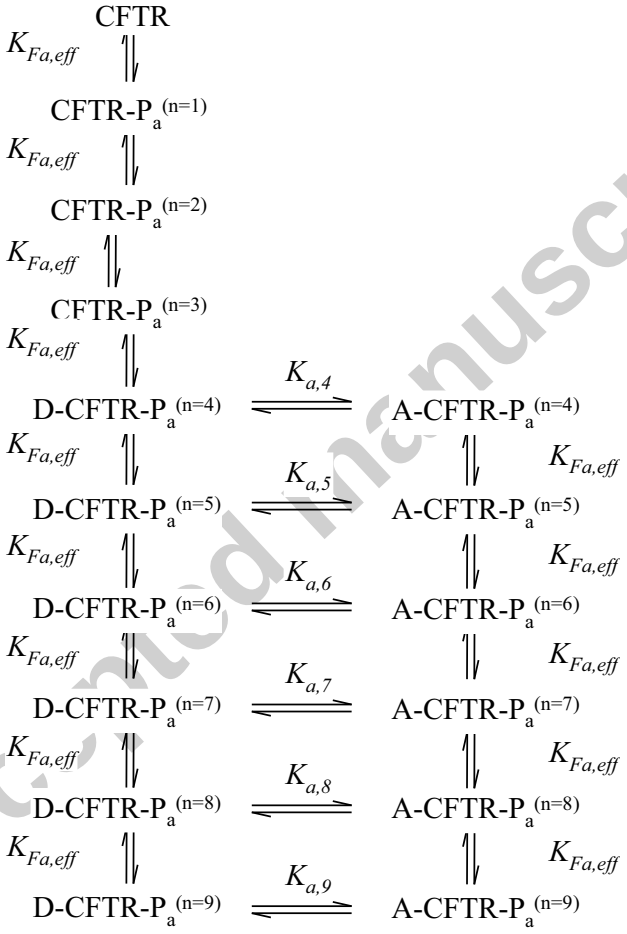

where D-CFTR-$P_a^{(n)}$ are the sequential phosphorylated-deactivated states, with n indicating the number of phosphorylated sites, and A-CFTR-$P_a^{(n)}$ are the corresponding activated states. The total probability to be in a given phosphorylated state is defined by:

$$CFTR - P_a^{(n)} = D - CFTR - P_a^{(n)} + A - CFTR - P_a^{(n)} \quad (4)$$

Sequential phosphorylation steps have the same equilibrium constant $K_{Fx,eff}$, where $1 \leq n \leq 9$, and n

is the number of phosphorylated activatory sites,

$$K_{Fa,eff} = \frac{CFTR - P_a^{(n)}}{CFTR - P_a^{(n-1)}} \tag{5}$$

Thus, the probability to be phosphorylated at least in one site, $CFTR\text{-}P_a^{(n>0)}$, depends on K_{Fa}, PKA_A, and to the ATP concentration. However, as the affinity of PKA for ATP is so high, no significant effect on the CFTR phosphorylation is seen for concentrations > 0.05 mM.

Distribution of phosphorylation states, i.e., the number of sites actually phosphorylated is defined by:

$$\begin{aligned}
CFTR - P_a^{(n=0)} &= \frac{(K_{Fa,eff})^9}{\sum_{n=0}^{9}(K_{Fa,eff})^n} \\
CFTR - P_a^{(n=1)} &= \frac{(K_{Fa,eff})^8}{\sum_{n=0}^{9}(K_{Fa,eff})^n} \\
&\vdots \\
CFTR - P_a^{(n=8)} &= \frac{K_{Fa,eff}}{\sum_{n=0}^{9}(K_{Fa,eff})^n} \\
CFTR - P_a^{(n=9)} &= \frac{1}{\sum_{n=0}^{9}(K_{Fa,eff})^n}
\end{aligned} \tag{6}$$

that is,

$$CFTR - P_a^{(n)} = \frac{(K_{Fa,eff})^{(9-n)}}{\sum_{n=0}^{9}(K_{Fa,eff})^n} \tag{7}$$

where $CFTR\text{-}P^{(n)}$ is the probability to have n sites phosphorylated. To be active, CFTR must have at least 4 sites phosphorylated, that is $n \geq 4$. The transition from the deactive state to the active state, $K_{a,n}$, become more favourable to the active state as the number of phosphorylated state increase (Vais et al, 2004):

$$K_{a,n} = \frac{A-CFTR-P_a^{(n)}}{D-CFTR-P_a^{(n)}} \tag{8}$$

where ξ_a is an "acceleration factor", i.e., a factor by which the activated conformation is favoured by increasing the phosphorylated sites; thus, for each transition the effective equilibrium constant is given by $K_{a,n} = K_a \xi_a (n-3)$. The total activated CFTR will be the defined as:

$$A-CFTR_{total} = \sum_{n=4}^{9} \left[CFTR-P_a^{(n)} \frac{K_{a,n}^{(effec)}}{1+K_{a,n}^{(effec)}} \right] \tag{9}$$

2.3 cAMP dependent phosphorylation of CFTR: inhibitory sites

Phosphorylation of the inhibitory sites is described by:

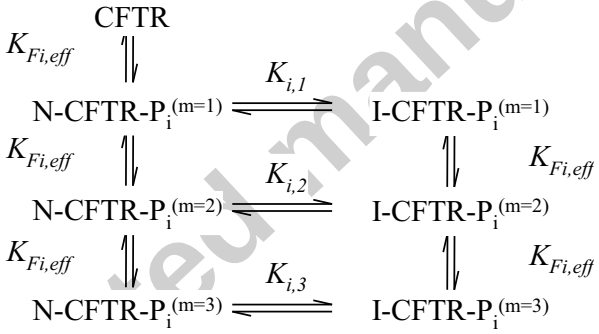

In this scheme, N-CFTR-$P_i^{(m)}$ are the sequential phosphorylated-non-inhibiting states, with m indicating the number of phosphorylated sites, and I-CFTR-$P_i^{(m)}$ are the corresponding inhibiting states. Successive phosphorylation steps have the same equilibrium constant,

$$K_{Fi,eff} = \frac{[CFTR-P_i^{(m-1)}]}{[CFTR-P_i^{(m)}]} \tag{10}$$

and the distribution of phosphorylated states is defined by:

$$CFTR-P_i^{(m)} = \frac{(K_{Fi,eff})^{(3-m)}}{\sum_{m=0}^{9} (K_{Fi,eff})^m} \tag{11}$$

The transition from the non-inhibiting state to the inhibiting state, K_i, become more favourable to the inhibiting state as the number of phosphorylated state increase:

$$K_{i,m} = K_i \xi_i (m-3) = \frac{I-CFTR-P_i^{(m)}}{N-CFTR-P_i^{(m)}} \tag{12}$$

where ξ_i is an "acceleration factor", i.e., a factor by which the inhibiting conformation is favoured by increasing the phosphorylated sites, as for the activation sites. The total inhibiting phosphorylated sites are defined as:

$$I-CFTR_{total} = \sum_{m=i}^{3} \left[CFTR-P_i^{(m)} \frac{K_{i,m}^{(effec)}}{1+K_{i,m}^{(effec)}} \right] \tag{13}$$

Considering both pathways, activation and inactivation, the probability of CFTR to be available for becoming permeable, $CFTR_{available}$, will be:

$$CFTR_{available} = A-CFTR_{total}\left(1-\Phi \times I-CFTR_{total}\right) \tag{14}$$

where ϕ the maximun fraction of inhibition obtained by phosphorylation of the inhibitory sites, to limit the inhibitory character of $I\text{-}CFTR_{total.}$

2.4 Gating of CFTR by ATP

When activated, CFTR serves as an anion channel gated by the binding of ATP to the nucleotide binding domains (NBDs). To open the channel, ATP must be bound to both domains, NBD1 and NBD2, according to the scheme:

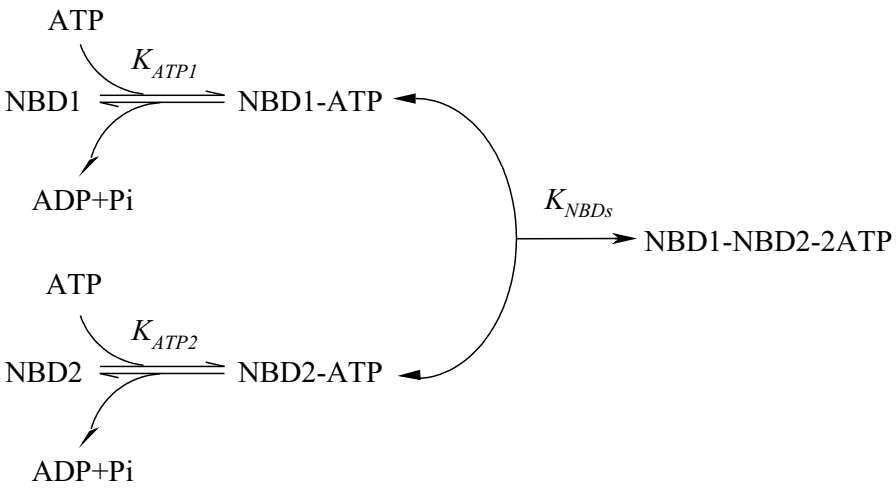

where K_{ATP1} and K_{ATP2} are the equilibrium constant of these transitions. Binding of ATP to both NBDs promote the "dimerisation" of them, that is correlated with the open (permeable) conformation of the CFTR anion channel (Vergani et al, 2005). Dimerisation is strongly favoured by ATP binding, and consequently the equilibrium constant of this transition $K_{NBDs} < 1$. While it is widely accepted that each NBD can bind one molecular of ATP independently, hydrolysis of ATP in NBD1 is believed to be strongly reduced, thus, defining the backward transition very slow. The probability to bind an ATP for the jth NBD is:

$$NBD_j - ATP = \frac{[ATP]}{[ATP] + K_{ATPj}} \tag{16}$$

The binding site of ATP on each NBD requires the contribution of the partner domain (Moran et al, 2005). Disruption of the binding site on NBD1 and NBD2 by mutations R555K and T1246N, respectively, yield an approximation of the independent equilibrium constants, K_{ATP1} = 71 μM and K_{ATP2} = 261 μM (Vergani et al 2005). Therefore, the fraction of activated channels that will be gated to the open, conductive, state expected for a cell with the standard intracellular ATP concentration (4.7 mM) is:

$$F_{NDB} = \frac{K_{NBDs}\left(NBD_1 - ATP \times NBD_2 - ATP\right)}{K_{NBDs} + 1} \tag{17}$$

and the fraction of permeable channels, to open and transport anions is:

$$CFTR_{permeable} = CFTR_{available} \times F_{NBD} \tag{18}$$

3. Properties of the CFTR model

To describe the general behaviour of the model I have used the values sumarised in Table 1, described on the previous section. There, values indicated with the asterisk has been obtained from experimental data reported in the literature (see above). Other values has been imposed and would need further experiments to assess their validity. Using these first set of values, I calculated the model responses shown in figure 2.

This model, as a function of intracellular cAMP and ATP concentration, is described by 13 parameters, 4 of them, K_d, K_P, K_{ATP2} and K_{ATP2} having some experimental basis, and other 9 parameters that are unknown. To examine the relative importance of these parameters I calculated the fraction of permeable CFTR channels as a function of the intracellular concentration of cAMP with different combinations of parameters. For each cAMP concentration, I calculated the apparent equilibrium constant, $K_{d,app}$, and the asymptotic maximum fraction of permeable CFTR channels, $CFTR_{permeable}^{(max)}$ assuming a simple first order kinetics for the dose-response curves (Moran and Zegarra-Moran, 2005).

The steady-state equilibrium constants for the phosphorylation-dephosphorylation reaction, $K_{F,a}$ and $K_{F,i}$, in Figure 2A were set identical for the activating and inhibiting sites. An increase of these parameters, that represent a favouring of phosphorylation, increase $K_{d,app}$ and $CFTR_{permeable}^{(max)}$. For $K_{F,a}$ and $K_{F,i}$ from 0.8 to 1.1 the $K_{d,app}$ yields values between 67 and 40 μM, that is the interval reported measuring the CFTR activity on cell monolayers (Moran and Zegarra-Moran, 2005). In this interval of $K_{F,a}$ and $K_{F,i}$, $CFTR_{permeable}^{(max)}$ shows more than two-fold variation, from 0.2 to 0.45. Variation of $CFTR_{permeable}^{(max)}$ is even larger, from less than 0.05 to more than 0.6, for larger changes of $K_{F,a}$ and $K_{F,i}$, as shown in Figure 2A.

The equilibrium constant for the transition from a phosphorylated-deactivated to an activated state, K_a, does induce significant changes on $CFTR_{permeable}^{(max)}$, from 0.13 to 0.49 for the interval of K_a analysed in Figure 2B. Similar variations of the equilibrium constant for the transition to the inhibiting state, K_i, do not modify significantly $CFTR_{permeable}^{(max)}$, but produce a reduction of $CFTR_{permeable}$ as K_i increases . Conversely, changes of both K_a or K_i cause a modest change of $K_{d,app}$, varying from 45 to 58 μM, i.e., in an interval described in Figure 2B. Similarly, variations of the "acceleration" factor of the transition from the phosphorylated-deactivated to the activated states, ξ_a, significantly modify $CFTR_{permeable}^{(max)}$ accompanied by modest changes on $K_{d,app}$ (Figure 2C).

Differently, the magnitude of the "acceleration" for the inhibiting states, ξi, has virtually no influence on $K_{d,app}$, and a modest influence (<0.05) in $CFTR_{permeable}^{(max)}$ (data not shown).

The equilibrium constants of the ATP binding to the NBDs, K_{ATP1} and K_{ATP2}, do not influence the $K_{d,app}$, and produce a little reduction of $CFTR_{permeable}^{(max)}$ (from 0.31 to 0.38, and from 0.33 to 0.39, for K_{ATP1} and K_{ATP2}, respectively), and any modification of $K_{d,app}$ for a change on the equilibrium constants from 5 μM to 1 mM (data not shown). Differently, a modification of the equilibrium constants for NBDs dimerisation, K_{NBDs}, produces a strong variation of $CFTR_{permeable}^{(max)}$, from 0.13 to 0.40 for a K_{NBDs} interval from 0.5 to 25 (Figure 2D). However, these changes on K_{NBDs} do not yield any modification on $K_{d,app}$. In this model, these data is accordant with the idea that the transition that leads to dimerisation of the NBDs does not influence the $K_{d,app}$. Changes in the intracellular ATP will determine the $CFTR_{permeable}^{(max)}$, as dimerisation is strongly influenced by the binding of ATP to the NBDs, but does nor modify $K_{d,app}$, except for low ATP, affecting the phosphorylation steps (Figure 4). Indeed, the slope of the decay of $K_{d,app}$ in Figure 4 is tightly dependent on the equilibrium constants of the phosphorylation reaction, K_p.

4. Action of CFTR potentiators predicted by the model

Most CFTR potentiators exert three actions on the target channel: 1) at low concentration, there is an increase the ion transport, by augmenting the ion channel open probability; 2) there is an inhibition of CFTR transport at high concentration of potentiator; 3) there is an increase of the response to cAMP as function of the potentiator concentration (Cai and Sheppard, 2002; Caci et al., 2003; Moran et al., 2005; Moran and Zegarra-Moran, 2005; Ferrera et al, 2007; Zegarra-Moran et al, 2007). Assuming that activatory and inhibitory actions of a potentiator are two separate phenomena, i.e., the drug wield its action at two different points in the activatory pathway, the most obvious candidates for the activatory effect of a potentiator are the steady-state equilibrium constants for the phosphorylation-dephosphorylation reaction, $K_{F,a}$ and $K_{F,i}$. As shown in Figure 3A, changes on these two parameters (or, at least, on the sole $K_{F,a}$), lead to a significant change of both, the sensitivity to cAMP stimulation and CFTR transport capacity. On the other hand, assuming that the inhibitory effect of the potentiator does not affect $K_{d,app}$, the best candidate to account for this effect is the dimerisation of the NBDs, by modifying the equilibrium constant K_{NBDs}.

To simulate the effect of a potentiator, $K_{F,a}$ and K_{NBDs} were varied as a function of the drug concentration, *POT*. The initial value of $K_{F,a}$ (for *POT* = 0), $K_{F,a}^{(0)}$, was set to 1, and its maximum

asymptotic value (for $POT \rightarrow \infty$), $K_{F,a}^{(\infty)}$, was set to 2.5. The dissociation constant for the potentiator in the activation site, $K^{(activ)}$ was set to 15. For the inhibitory effect of the potentiator, the initial value of K_{NBDs} was set to $K_{NBDs}^{(0)} = 8$. and the dissociation constant for the potentiator in the inhibitory site, $K^{(inhib)}$ was set to 100. Consequently, the values for $K_{F,a}$ and K_{NBDs} as a function of *POT* was evaluated as:

$$K_{F,a} = 1 + \left(K_{F,a}^{(\infty)} - 1\right) \frac{POT}{POT + K^{(activ)}} \tag{19}$$

$$K_{NBDs} = K_{NBDs}^{(0)} \frac{K^{(inhib)}}{POT + K_{inh}} \tag{20}$$

The results of this simulation is shown in Figure 5. The parameter $K_{F,a}$ increases as a function of *POT,* while K_{NBDs} decreases (Figure 5A). The result of this behaviour is an initial increase of $CFTR_{permeable}$ at low potentiator concentration, and a successive inhibition of the permeability as *POT* is further increased (Figure 5B). Moreover, the slope of the initial part of the $CFTR_{permeable}$-*POT* curve becomes steeper, as well as the decay of the curve at high potentiator concentration, as the cAMP concentration is increased. These properties clearly resemble those experimentally obtained for several potentiators (Moran et al., 2005; Moran and Zegarra-Moran, 2005; Ferrera et al, 2007; Zegarra-Moran et al, 2007).

5. Discussion

CFTR is chloride channel with a complex regulation, whose malfunction causes cystic fibrosis. I present here a model of the activation and gating of CFTR. The model represents the steps hypothesed to cause the activation of CFTR by cAMP dependent phosphorylation, and the subsequent gating of the channel by ATP binding. The first step considered in the model is the intracellular increase of cAMP, as this event is routinelly used to investigate the pharmacology and physiology of CFTR in integral cell or cell monolayer preparations, either by activating the adenylate clyclase by forskolin, or by direct application of membrane permeable cAMP analogues (Moran and Zegarra-Moran, 2008). The model represents the equilibrium response of CFTR, and does not attempt to include the time course of the responses. This limitation is justified by the fact that while most relaxation times of the different steps in the pathway of activation and gating of CFTR are relatively fast (from millisecondsa to tens of seconds), CFTR-dependent ionic fluxes with a physiological relevance occur in minutes.

The model contains several assumptions, most due to the lack of information on different steps on the activatory pathway of CFTR. The outputs of the model are the probability to be activated and permeable (related to the ability of CFTR to transport ions), and the apparent equilibrium constant of cAMP. The former parameter is an extensive property of the system, that is difficult to directly correlate with experimental data, as the measurement of the anion transport will depend on the magnitude of the expression of CFTR in a given preparation. Differently, the apparent equilibrium constant of cAMP is an intensive property of the CFTR response. Hence, it was used as indicator to decide the magnitude of the unknown parameters of the model.

A series of simulations was done to find-out a parameter combination that results on a response to cAMP similar to experimental measurements. It is interesting to observe that the phosphorylation/dephosphorylation equilibrium, $K_{f,a}$ and $K_{f,i}$ (equation 2), is the most sensible parameter of the system, which can cause important changes on the cAMP responses as well as on the maximum ion transport of the system (see Fig. 3A). Differently, the equilibrium of the (phosphorylated) activated and inactivated states, represented by K_a and K_i, or by the "acceleration factor" ξ_a, have a strong influence on the apparent cAMP equilibrium constant, but a reduced effect on the maximun CFTR activity (see Figs 3B and 3C). Conversely, according to this model, the ATP-dependent gating of CFTR is about independent of the apparent cAMP equilibrium constant, affecting significantly only the maximum CFTR activity (Fig. 3D).

Development of drugs that increase the CFTR transport activity, named "potentiators", is considered of prime importance for the future treatment of cystic fibrosis, either improving the hypofunctioning phenotypes (class 3 and class 4 mutations), or coadjuvating the pharmacological rescue of channels with class 2 mutations with "correctors". Using this model, and based on the properties of the CFTR potentiators so far described, I have tried to find out the conditions to simulate the effect of these drugs. We have previously suggested that potentiators act by binding the NBDs, exerting its activatory and inhibitory actions in the same site (Moran et al, 2005; Moran and Zegarra-Moran, 2006; Zegarra-Moran et al, 2007), that would be related to the dimerisation equilibrium constant, K_{NBDs}. According to this model, it is unlikely that modification of K_{NBDs} leads to an activation concomitant to a change in the equilibrium constant of cAMP, as observed experimentally. Thus, binding of a potentiator to the NBDs would be responsible to the inhibition effect of the drug. In this framework, the only parameter that could account for a concomitant increase of CFTR activity, and a reduction of the apparent cAMP equilibrium constant is the phosphorylation/dephosphorylation constant, favouring the phosphorylated state of CFTR. It remains, indeed, the question whether a potentiator favours a phosphorylation of the regulatory domain, or it inhibits the dephosphorylation

of CFTR. Another point that cannot be immediately solved is whether the action of the potentiator is exerted on the catalysing enzymes, protein kinase-A or phosphatase, or it causes a modification on the regulatory domain that renders it more easy to be phosphorylated (or difficult to be dephosphorylated). This last hypothesis cannot be discarded a priori in view of the changes on the potentiator equilibrium constants by CFTR mutations (Moran et al, 2005).

The model of activation and gating of CFTR presented here is capable to reproduce the characteristics of a potentiator. The model yields a potentiator mechanism of action that is in contrast to that proposed previously. This novel proposal, that needs, indeed, a series of experimental tests to support the model, may represent an excellent framework to plan functional experiments for the design and develop of CFTR potentiator drugs.

Acknowledgements: Supported by Fondazione per la Ricerca sulla Fibrosi Cistica (grant FFC#2/2008) with the contribution of: Mille bambini a Via Margutta - onlus, Blunotte, Lega Italiana FC - Associazione Toscana

References

Button, B., Reuss, L., Altenberg, G.A., 2001. Pkc-mediated stimulation of amphibian cftr depends on a single phosphorylation consensus site. insertion of this site confers pkc sensitivity to human cftr. J. Gen. Physiol. 117, 457-468.

Caci, E., Folli, C., Zegarra-Moran, O., Ma, T., Springsteel, M.F., Sammelson, R.E., Nantz, M.H., Kurth, M.J., Verkman, A.S., and Galietta, L.J., 2003. CFTR activation in human bronchial epithelial cells by novel benzoflavone and benzimidazolone compounds. Am J Physiol Lung Cell Mol Physiol 285, L180-L188.

Cai, Z., and Sheppard, D.N., 2002. Phloxine B interacts with the cystic fibrosis transmembrane conductance regulator at multiple sites to modulate channel activity. J Biol Chem 277, 19546-19553.

Chang, X. B., Tabcharani, J. A., Hou, Y. X., Jensen, T. J., Kartner, N., Alon, N., Hanrahan, J. W., and Riordan, J. R. (1993) Protein kinase A (PKA) still activates CFTR chloride channel after mutagenesis of all 10 PKA consensus phosphorylation sites, J Biol Chem 268, 11304-11311.

Chappe, V., Hinkson, D.A., Howell, L.D., Evagelidis, A., Liao, J., Chang, X., Riordan, J.R., Hanrahan, J.W., 2004. Stimulatory and inhibitory protein kinase c consensus sequences regulate the cystic fibrosis transmembrane conductance regulator. Proc. Natl. Acad. Sci. U.S.A. 101, 390-395.

Csanady, L., Seto-Young, D., Chan, K. W., Cenciarelli, C., Angel, B. B., Qin, J., McLachlin, D. T., Krutchinsky, A. N., Chait, B. T., Nairn, A. C., and Gadsby, D. C. (2005) Preferential phosphorylation of R-domain Serine 768 dampens activation of CFTR channels by PKA, J Gen Physiol 125, 171-186

Dao, K.K., Teigen, K., Kopperud, R., Hodneland, E., Schwede, F., Christensen, A.E., Martinez, A., and Doskeland, S.O., 2006. Epac1 and cAMP-dependent protein kinase holoenzyme have similar cAMP affinity, but their cAMP domains have distinct structural features and cyclic nucleotide recognition. J Biol Chem 281, 21500-11.

Ferrera, L., Pincin, C., and Moran, O., 2007. Characterization of a 7,8-Benzoflavone Double Effect on CFTR Cl(-) Channel Activity. J Membr Biol 220, 1-9.

Galietta, L.J., and Moran, O., 2004. Identification of CFTR activators and inhibitors: chance or design? Curr Opin Pharmacol 4, 497-503

James, A. M., Sheard, P. W., Wei, Y. H., and Murphy, M. P. 1999. Decreased ATP synthesis is phenotypically expressed during increased energy demand in fibroblasts containing mitochondrial tRNA mutations, European journal of biochemistry / FEBS 259, 462-469.

King, J.D.J., Fitch, A.C., Lee, J.K., McCane, J.E., Mak, D.D., Foskett, J.K., Hallows, K.R., 2009. Amp-activated protein kinase phosphorylation of the r domain inhibits pka stimulation of cftr.

Am. J. Physiol., Cell Physiol. 297, C94-101.

Kongsuphol, P., Cassidy, D., Hieke, B., Treharne, K.J., Schreiber, R., Mehta, A., Kunzelmann, K., 2009. Mechanistic insight into control of cftr by ampk. J. Biol. Chem. 284, 5645-5653.

Moran, O., Galietta, L. J. V., and Zegarra-Moran, O. 2005. Binding site of activators of the cystic fibrosis transmembrane conductance regulator in the nucleotide binding domains, Cell. Mol. Life Sci. 62, 446–460.

Moran, O., and Zegarra-Moran, O., 2005. A quantitative description of the activation and inhibition of CFTR by potentiators: Genistein. FEBS Lett 579, 3979-83.

Moran, O., and Zegarra-Moran, O., 2008. On the measurement of the functional properties of the CFTR. J Cyst Fibros 7, 483-94.

Seavilleklein, G., Amer, N., Evagelidis, A., Chappe, F., Irvine, T., Hanrahan, J.W., Chappe, V., 2008. Pkc phosphorylation modulates pka-dependent binding of the r domain to other domains of cftr. Am. J. Physiol., Cell Physiol. 295, C1366-75.

Seibert, F. S., Chang, X. B., Aleksandrov, A. A., Clarke, D. M., Hanrahan, J. W., and Riordan, J. R., 1999. Influence of phosphorylation by protein kinase A on CFTR at the cell surface and endoplasmic reticulum, Biochimica et biophysica acta 1461, 275-283.

Vais, H., Zhang, R., and Reenstra, W. W., 2004, Dibasic phosphorylation sites in the R domain of CFTR have stimulatory and inhibitory effects on channel activation, Am J Physiol Cell Physiol 287, C737-745

Vergani, P., Lockless, S. W., Nairn, A. C., and Gadsby, D. C., 2005. CFTR channel opening by ATP-driven tight dimerization of its nucleotide-binding domains, Nature 433, 876-880.

Zegarra-Moran, O., Monteverde, M., Galietta, L.J., and Moran, O., 2007. Functional analysis of mutations in the putative binding site for cystic fibrosis transmembrane conductance regulator potentiators. Interaction between activation and inhibition. J Biol Chem 282, 9098-104.

Zu, Y. L., Wu, F., Gilchrist, A., Ai, Y., Labadia, M. E., and Huang, C. K., 1994. The primary structure of a human MAP kinase activated protein kinase 2, Biochemical and biophysical research communications 200, 1118-1124

Captions to the figures.

Figure 1. Schematic representation of the pathway to activate and gate the CFTR anion channel.

Figure 2**.** Behaviour of the CFTR steady-state model as a function of the intracellular cAMP concentration, calculated with the parameters described in Table 1. **A**: Probability to be phosphorylated at the activating state. Broken lines represents the no-phosphorylated state ($n = 0$; black) and states $n = 1$ to 3 (red, orange and yellow), that cannot undergo activation. Other states, that can undergo activation ($n \geq 4$), are represented by continuous lines (green, blue, cyan, violet, magenta and pink, respectively). **B**: Probability to be phosphorylated at the inactivating states. The no-phosphorylated state ($m = 0$) is represented by the broken line (black), and the phosphorylated inactivating states ($m \geq 1$) are represented by the continuous lines (red, green and blue). **C**: Probability that a phosphorylated activating site leads to a CFTR active state, for $n \geq 4$. Traces have the same colours as in **A**. **D**: Probability of the totally activated CFTR (black), contribution of the phosphorylated inhibiting sites (blue), the actually activated CFTR, after subtracting the contribution of the inhibiting sites (red), and the probability to be in the open permeable state (green).

Figure 3. The apparent equilibrium constant of cAMP, $K_{d,app}$ (red) and the maximum fraction of permeable CFTR channels, $CFTR^{(max)}_{permeable}$, (blue) as a function of $K_{F,a}$ and $K_{F,i}$ (**A**), K_a and K_i (**B**), ξ_a (**C**), and K_{NBDs} (**D**). Other parameters where kept as shown in Table 1. The inset on each panel is the fraction of permeable CFTR channels as a function of *cAMP* evaluated for three values of the corresponding parameter, as indicated in the figure.

Figure 4**.** The apparent equilibrium constant of cAMP, $K_{d,app}$ (red) and the maximum fraction of permeable CFTR channels, $CFTR^{(max)}_{permeable}$, (blue) as a function of intracellular ATP concentration.

Figure 5. Simulation of the effect of a potentiator on CFTR. A: KF,a (blue) and KNBDs (red) as a function of the potentiator concentration. B: the CFTR activity, CFTRpermeable, as a function of the potentiator concentration, evaluated for 10 (magenta), 20 (black), 50 (blue) and 100 (green) μM cAMP. The apparent equilibrium constant for cAMP calculated as a function of the potentiator concentration is shown in red. Parameters for the evaluation of these curves are described in the text.

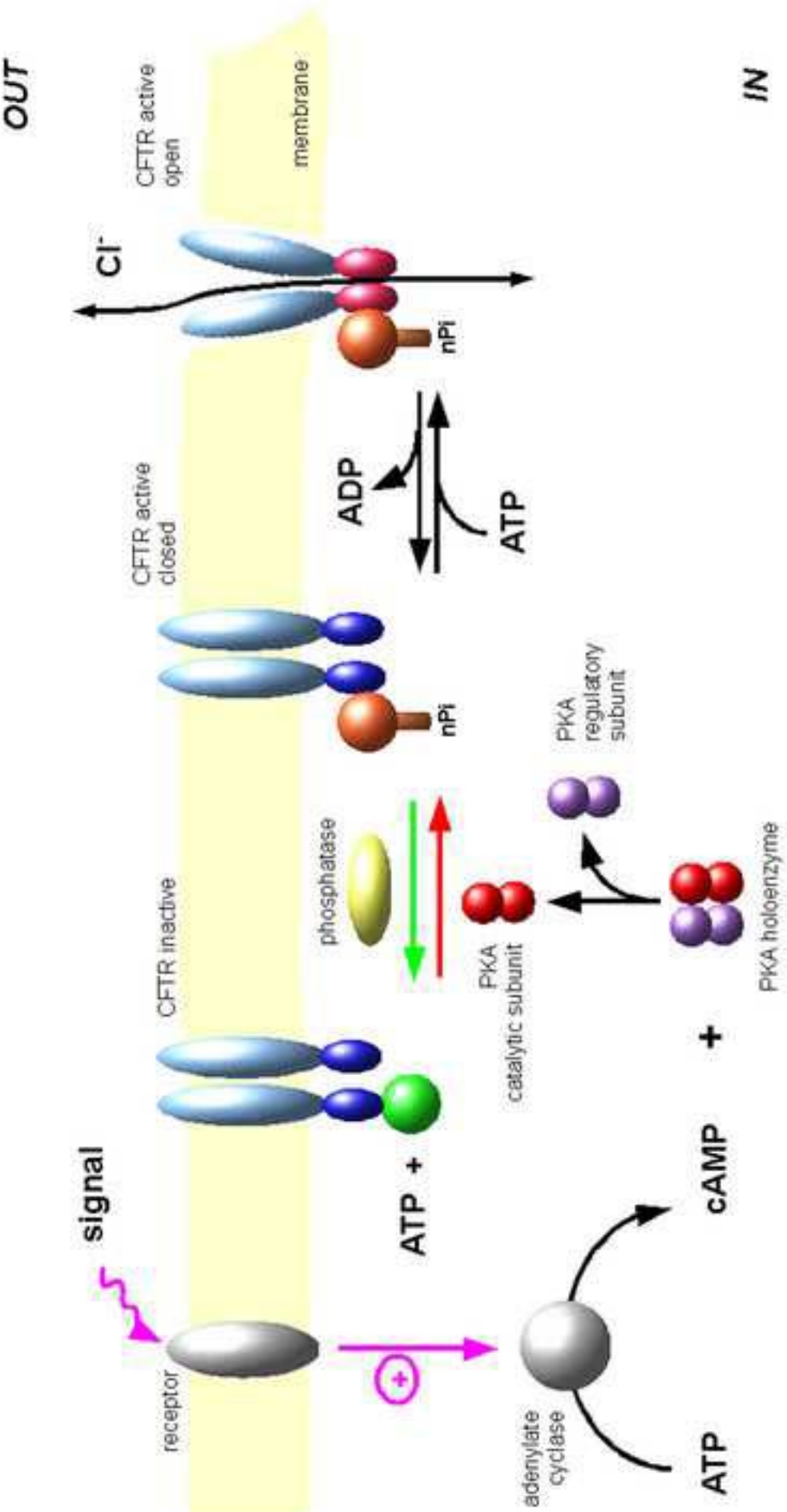

Figure 1

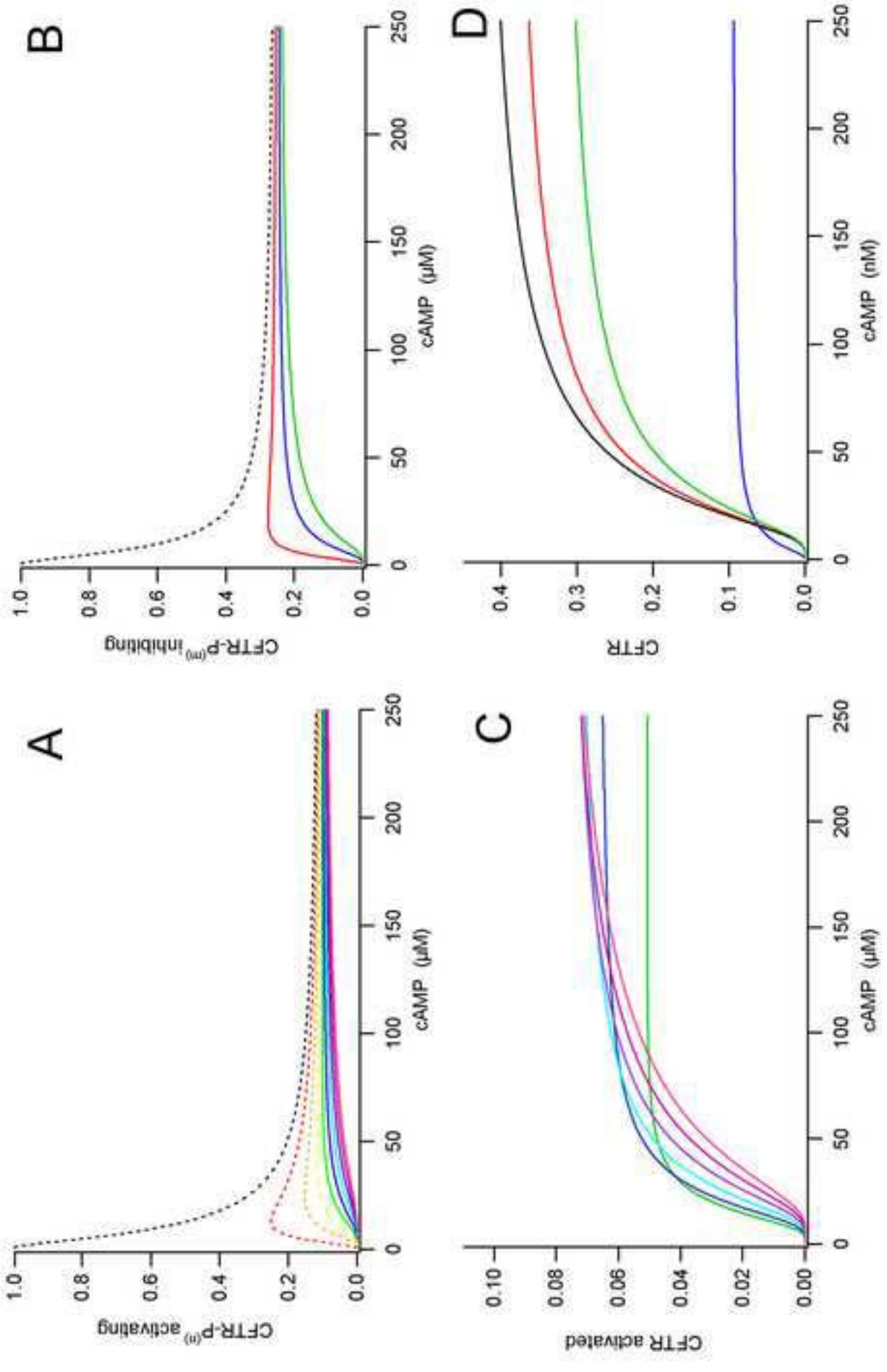

Figure 2

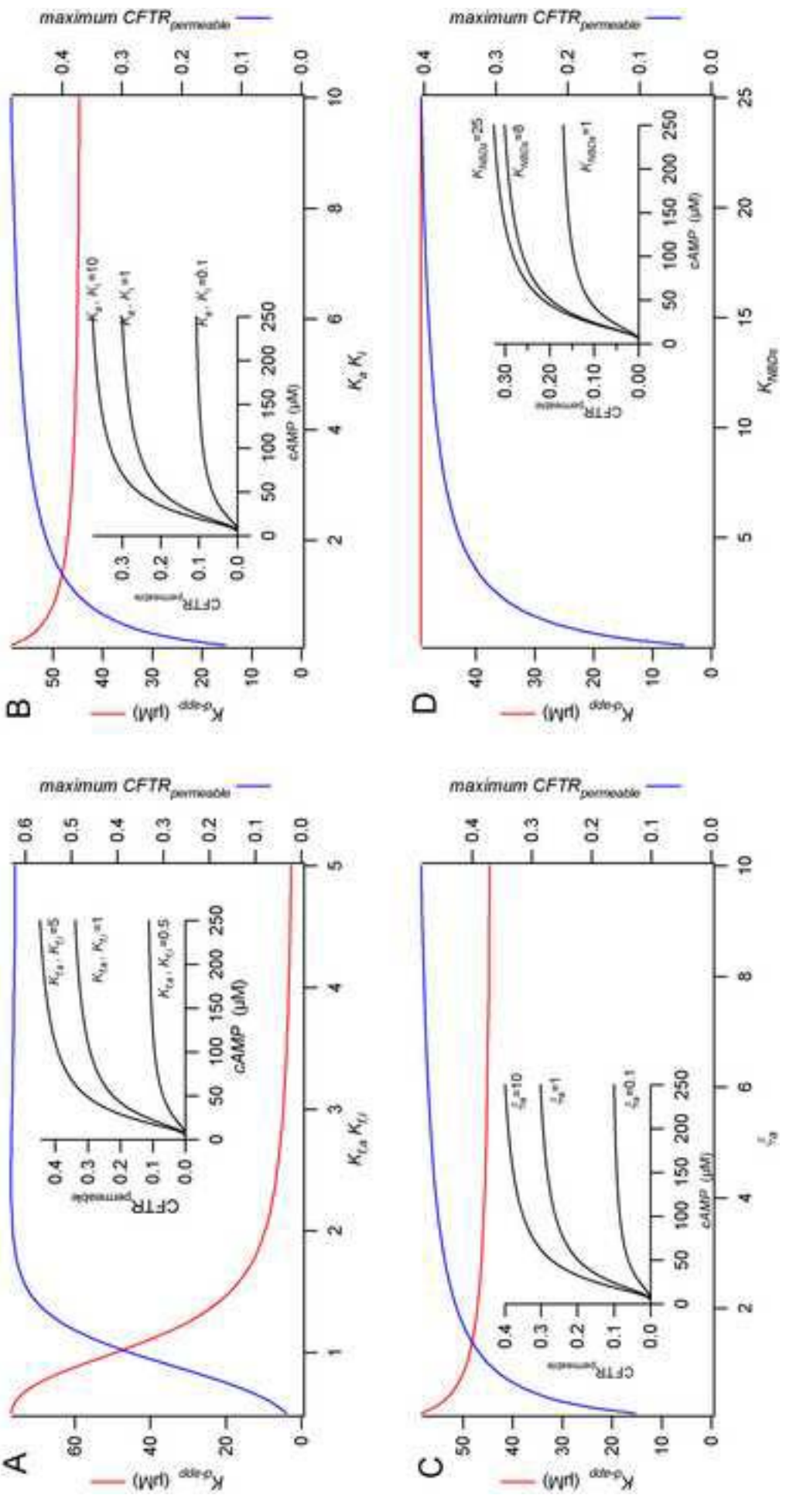

Figure 3

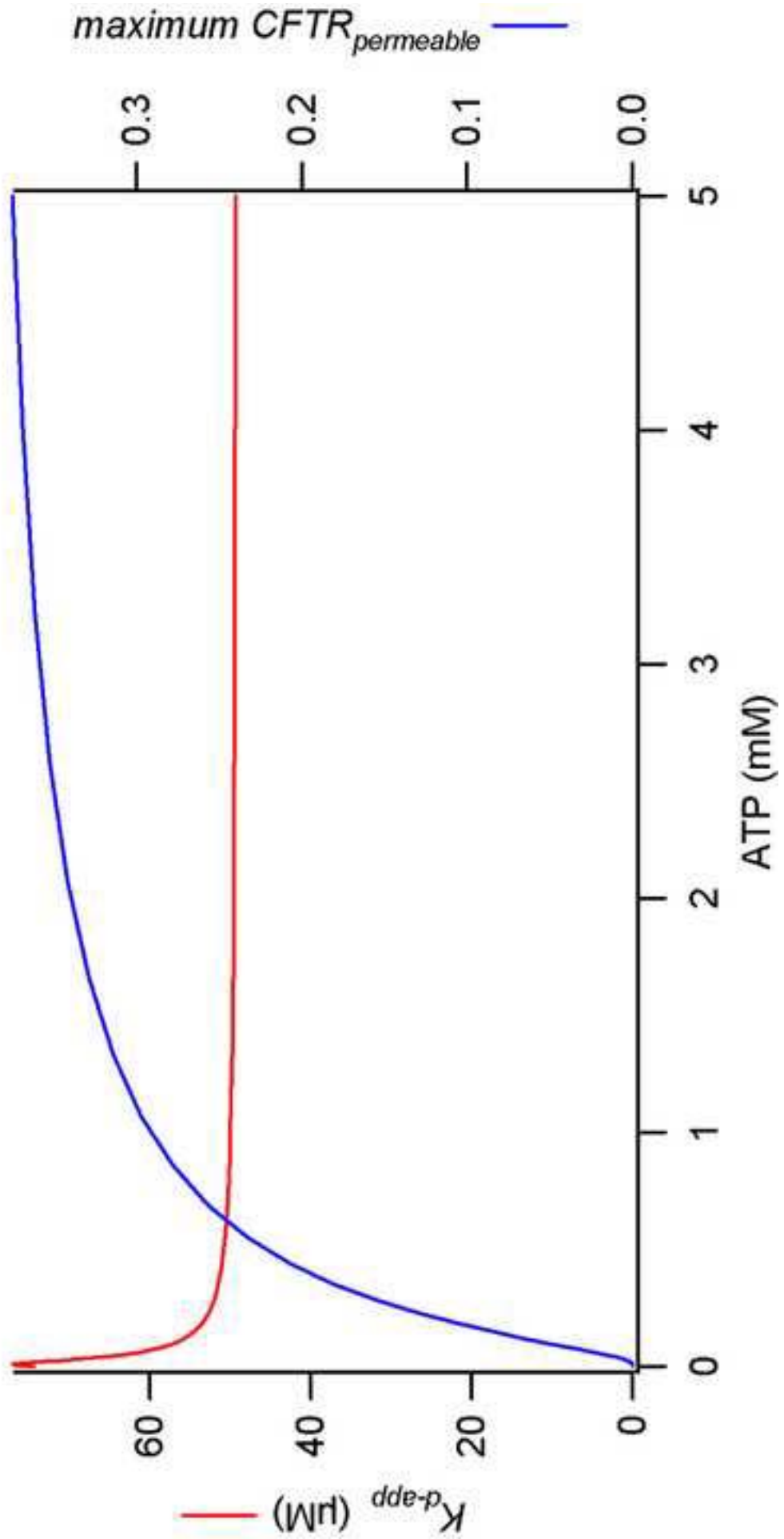

Figure 4

Figure 5

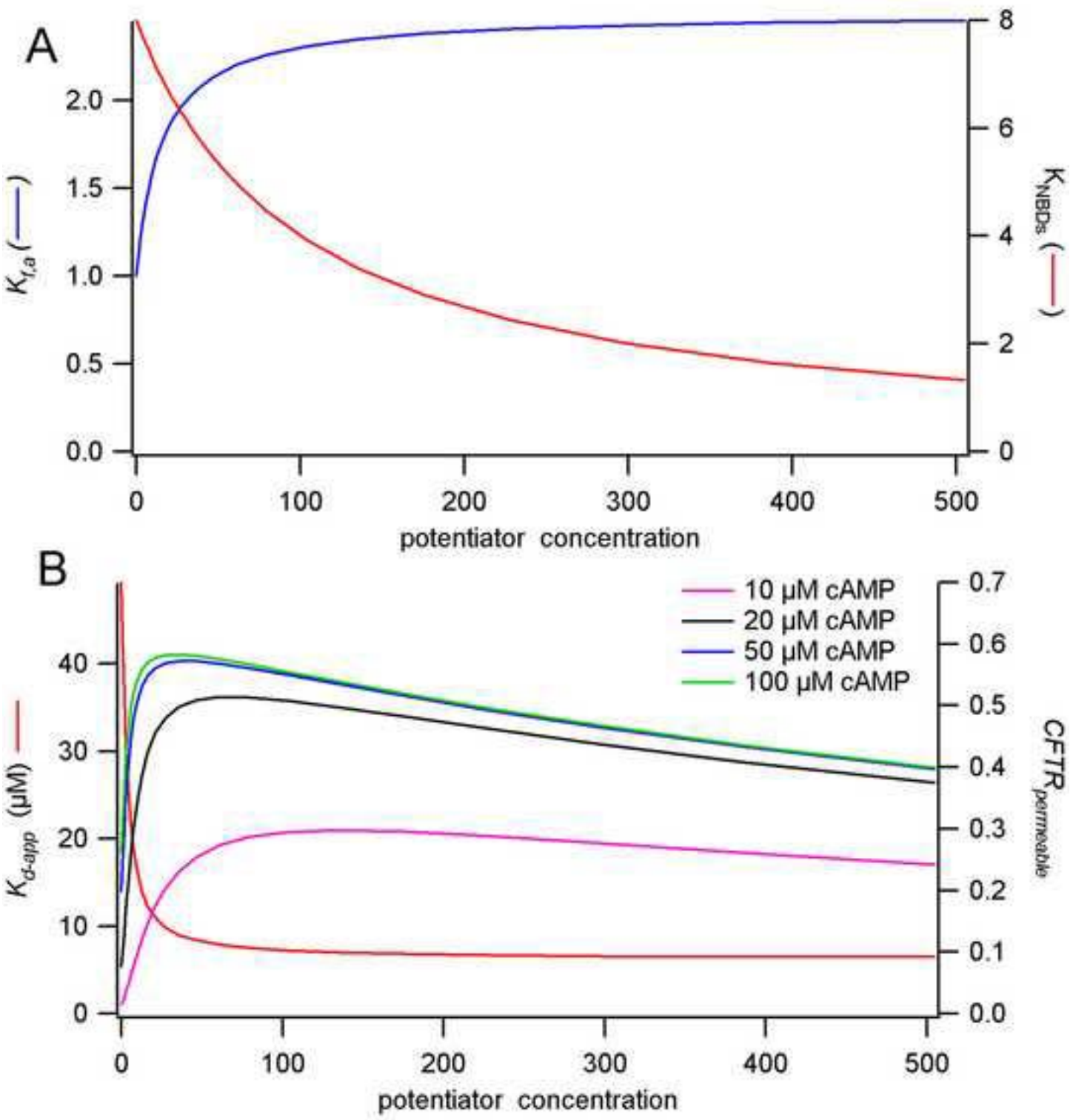

Table 1. Initial parameters used to evaluate the CFTR model, used to construct figure 2.

K_d * (μM)	np	K_P * (μM)	$K_{F,a}$	K_a	ξ_a	$K_{F,i}$	K_i	ξ_i	Φ	K_{ATP1}* (μM)	K_{ATP2}* (μM)	K_{NBD_s}	ATP * (mM)
2.4	4	9.3	1	1	1	1	1	1	0.2	71	261	8	4.7